Heterotrophic and Photoautotrophic Media Optimization Using Response Surface Methodology for the Novel Microalga *Chlorococcum amblystomatis*

Nádia Correia [1,2,3], Hugo Pereira [4], Peter S. C. Schulze [4], Monya M. Costa [4], Gonçalo E. Santo [2], Inês Guerra [2], Mafalda Trovão [2,4], Ana Barros [2], Helena Cardoso [2], Joana L. Silva [2], Luísa Gouveia [3,4] and João Varela [1,4,*]

1   CCMAR—Centro de Ciências do Mar, Campus de Gambelas, University of Algarve, 8005-139 Faro, Portugal
2   Allmicroalgae Natural Products S.A., Research and Development Department-Rua 25 de Abril, 2445-413 Alcobaça, Portugal
3   LNEG—Laboratório Nacional de Energia e Geologia I.P., Bioenergy and Biorefineries Department, Estrada do Paço do Lumiar 22, 1649-038 Lisbon, Portugal
4   GreenCoLab-Associação Oceano Verde, Campus de Gambelas, Universidade do Algarve, 8005-139 Faro, Portugal
*   Correspondence: jvarela@ualg.pt; Tel.: +351-289-800-900; Fax: +351-289-800-069

Abstract: The nutritional requirements of novel microalgal strains are key for their effective cultivation and metabolite content. Therefore, the optimization of heterotrophic and photoautotrophic culture media is crucial for novel *Chlorococcum amblystomatis* growth. Heterotrophic and photoautotrophic biomass samples were characterized to identify the differences between their heterotrophic and photoautotrophic biomass composition and their biotechnological potential. Media optimization through surface response methodology led to 44.9 and 51.2% increments in *C. amblystomatis*-specific growth rates under heterotrophic and photoautotrophic growth, respectively. This microalga registered high protein content (61.49–73.45% dry weight), with the highest value being observed in the optimized photoautotrophic growth medium. The lipid fraction mainly constituted polyunsaturated fatty acids, ranging from 44.47 to 51.41% for total fatty acids (TFA) in cells under heterotrophy. However, these contents became significantly higher (70.46–72.82% TFA) in cultures cultivated under photoautotrophy. An interesting carotenoids content was achieved in the cultures grown in optimized photoautotrophic medium: 5.84 mg·g^{-1} β-carotene, 5.27 mg·g^{-1} lutein, 3.66 mg·g^{-1} neoxanthin, and 0.75 mg·g^{-1} violaxanthin. Therefore, *C. amblystomatis* demonstrated an interesting growth performance and nutritional profile for food supplements and feed products that might contribute to meeting the world's nutritional demand.

Keywords: microalgae; *Chlorococcum amblystomatis*; growth optimization; response surface methodology; hetero- and photoautotrophic cultivation

1. Introduction

Alternative sources of nutrients and food ingredients rich in bioactive compounds have sparked great interest in the last years, particularly due to their benefits for human and animal health [1,2]. Microalgae can produce a wide range of metabolites such as proteins, lipids, carbohydrates, and valuable pigments with relevant bioactivities that can be used to enhance the nutritional value of food and feed, providing significant health benefits [3–5]. Furthermore, these micro-organisms have the great advantage of growing in industrial reactors, preventing their competition with food crops for fresh water supply and arable land. In addition, they can be harvested daily and offer higher reliability and even seasonal-independence, particularly if they are grown under controlled conditions indoors, as in heterotrophy [6–8]. Finally, microalgae industrial production still entails high production costs, and the scale-up of cultures from the laboratory scale to industrial photobioreactors is a highly time-consuming process that needs to be addressed [9].

Besides photoautotrophic growth, some microalgae species have the ability to grow heterotrophically using alternative metabolic pathways [10,11]. Heterotrophic cultivation implies the ability to grow in the absence of light, with organic carbon supplementation to replace light energy [12]. This type of cultivation appears to be an alternative to more economical industrial cultivation since it enables stricter control of the process parameters and higher growth rates, leading to cell concentrations in the order of 100 g·L^{-1} [11–14] and a reduction in harvesting costs [15]. Nevertheless, this cultivation mode decreases the protein and pigment contents in the resulting biomass [15]. According to *Barros* et al. [9], a two-stage approach, combining heterotrophic inoculum and photoautotrophic cultivation, might be an advantageous strategy to improve industrial production since it overcomes these limitations and provides high-quality biomass.

Moreover, increasing microalgae growth rates and biomass productivity while reducing operational costs is essential for the future of industrial producers. In addition, the production of different microalgal species is key to promoting a thorough portfolio of bioactive compounds. These compounds can be of interest for different biotechnological applications towards the development of sustainable and economical solutions for today's needs [16,17]. In addition, the appropriate culture medium recipes, a factor that is crucial for obtaining highly concentrated microalgal cultures, must be developed to enhance biomass and target metabolite productivities [18].

In order to achieve the aforementioned goal, the use and design of experiment methodologies has been applied, which allows for a reduction in time and the number of experiments and is more accurate than 'one variable at a time methods' since it evaluates interactions between the variables tested [19,20]. Response surface methodology (RSM) is a compilation of mathematical/statistical techniques that allow for the designing of experiments and the assessment of their effects and significance, and the monitoring of the interaction of several variables in specific responses through the evaluation of empirical models [21]. RSM has become a fundamental tool in numerous branches of scientific and technological research, such as biotechnology, namely in medium-optimization studies [22,23]. Therefore, the present work focused on the optimization of photoautotrophic and heterotrophic culture media for a novel microalga, previously known as *Oophila amblystomatis* and recently reclassified as *Chlorococcum amblystomatis* [24]. The biomass composition of *C. amblystomatis* was evaluated regarding protein, pigments, lipid, and carbohydrate contents to determine the nutritional profile attained in each cultivation condition.

2. Materials and Methods

2.1. Microalgal Strain and Growth Conditions

Chlorococcum amblystomatis was obtained from Allmicroalgae (Pataias, Portugal) culture collection.

Heterotrophic culture conditions: for the Plackett–Burman screening and Box–Behnken experiment, *Chlorococcum amblystomatis* axenic cultures were incubated in 250-mL Erlenmeyer flasks with 50 mL of culture medium that were placed on an orbital shaker (150 rpm, at 28 °C in the absence of light). The validation of medium optimization was performed under the same conditions.

Photoautotrophic culture conditions: for the Box–Behnken experiment, a heterotrophic *C. amblystomatis* culture was used to inoculate the photoautotrophic reactors. Axenic cultures were grown in 100 mL bubble columns with 30 mL of culture medium at 23 ± 1 °C with continuously injected compressed 0.2 µm filtered air under the continuous radiation of 100 µmol photons m^{-2}·s^{-1}. Optimal medium validation was performed in 1 L bubble column reactors with 0.8 L of culture medium, at 23 ± 1 °C with continuously injected compressed 0.2 µm filtered air under continuous radiation of 100 µmol photons m^{-2}·s^{-1}. pH was kept between 7.5 and 8.0 by CO_2 injection.

2.2. Growth Assessment

Microalgal growth was assessed by measuring dry weight (DW) until the cultures reached the stationary phase. Briefly, a defined sample volume was filtered on microglass filters (0.7 μm, VWR), washed with an equal volume of deionized water, and dried using a moisture analyzer (KERN DBS, KERN & Sohn GmbH, Balingen-Frommern, Germany) at 120 °C.

Volumetric biomass productivity (P) was calculated as the difference in biomass concentration (X) during a specific time (t), in $g \cdot L^{-1} \cdot h^{-1}$ for heterotrophy and in $g \cdot L^{-1} \cdot d^{-1}$ for photoautotrophy, following the Equation (1):

$$P = \frac{X_2 - X_1}{t_2 - t_1} \tag{1}$$

Specific growth rate (μ) was determined by the quotient between the linearized biomass concentration (X) within a period of time (t) in h^{-1} for heterotrophy and d^{-1} for photoautotrophy, as depicted in Equation (2):

$$\mu = \frac{\ln(X_2 / X_1)}{t_2 - t_1} \tag{2}$$

where X_2 and X_1 refer to biomass concentration in grams per liter, and t_2 and t_1 refer to different time points.

2.3. Experimental Design

The Plackett–Burman design was accomplished as a preliminary assay to evaluate the influence of two coded levels and two central points of temperature (T), vitamins, and thirteen nutrients on *Chlorococcum amblystomatis*-specific growth rate. Based on the company's basal medium, the lowest and highest concentration levels of vitamins, phosphorus, calcium, magnesium, iron, zinc, cobalt, molybdate, manganese, nickel, copper, boron, and nitrogen, as well as the nitrogen source, namely urea $((NH_2)_2CO)$ and ammonium sulfate $((NH4)_2SO_4)$, were set. The significance of each medium component towards the culture growth, mainly specific growth rates, was considered as the response variable, and the results of variance analysis were achieved using the Minitab® v.20 software.

Thereafter, a Response Surface Methodology was performed using Box–Behnken methodology to determine the optimal values of the significant factors resulting from the Plackett–Burman screening. The concentrations of non-significant factors were constant. To verify the model, the variance analysis was evaluated using Design-Expert® v.11 software, and the experimental-specific growth rates were compared with the predicted values given by the linear polynomial Equation (3), obtained from the model:

$$Y = a_0 + a_1 A + a_2 B + a_3 C + a_4 AB + a_5 AC + a_6 BC \tag{3}$$

where Y represents the specific growth rate value; A, B, and C correspond to the factors with significant effects on specific growth rates; a_0 is the intercept, and a_1–a_6 are the estimated coefficients.

2.4. Biochemical Composition

Total lipid content was determined according to the Bligh and Dyer [25] method with some modifications [26]. Briefly, approximately 20 mg of freeze-dried biomass was extracted with a mixture of chloroform, methanol, and water (1:2:0.8, *v:v:v*) and homogenized for 3 minutes in a mixer mill (MM400, Retsch GmbH, Retsch-Alle 1-5, 42781 Haan, Germany) with glass beads at 30 Hz. The chloroform layer, separated by centrifugation, was transferred to new vessels. Then, 0.7 mL were pipetted to preweighed tubes and evaporated at 60 °C. The resulting dried residue was weighed (Sartorius Lab Instruments GmbH & Co. 37070 Gottingen, Germany-MSA36S-000-DH) and compared with the initial weight to provide an accurate result of the lipid fraction.

Protein content was calculated by multiplying the N content with the standard conversion factor of 6.25 [27] after CHN analysis using a Vario EL III (Vario EL, Elementar Analyser System, GmbH, Hanau, Germany).

The ash content was determined by the biomass's weight difference before and after combustion. Biomass was heated at 550 °C for 8 h using a furnace (LE062K17N1, Nabertherm, Lilienthal, Germany).

Carbohydrates were determined by differences from other macronutrients.

Fatty acid methyl esters (FAME) were determined according to Lepage and Roy [28] protocol, modified by Pereira et al. [26]. Briefly, 20 mg of freeze-dried biomass was added to 1.5 mL of methanol/acetyl chloride (20:1 *v:v*) and homogenized for 3 minutes in a mixer mill (MM400, Retsch GmbH, Retsch-Alle 1-5, 42781 Haan, Germany) with glass beads, at 30 Hz. Then, 1 mL of *n*-hexane was added to the derivatization vessels and placed in a water bath (70 °C for 60 min). Thereafter, water and *n*-hexane (1:4, *v:v*) were added and homogenized in a vortex. The hexane fraction, obtained by centrifugation, was transferred to new tubes, and anhydrous sodium sulfate (Na_2SO_4) was added to the extracts. After filtration, samples were evaporated under nitrogen gas flow. The pellet was resuspended in 0.5 mL of gas chromatography-grade hexane and analyzed in a GC-MS analyzer (Bruker SCION 456/GC, SCION TQ MS) equipped with a ZB-5MS capillary column (30 m × 0.25 mm of internal diameter, 0.25 μm of film thickness, Phenomenex), using helium as the carrier gas. The temperature was set to 60 °C for 1 min, then 30 °C min^{-1} to 120 °C, 5 °C min^{-1} to 250 °C and finally increased to 20 °C min^{-1} up to 300 °C, with the injection temperature being 300 °C as well. To establish the calibration curves, five different concentrations of the standards Supelco® 37 component FAME Mix 41 (Sigma-Aldrich, Sintra, Portugal) were analyzed for further identification and quantification of FAME.

For chlorophylls *a* and *b* quantification, 10 mg of freeze-dried biomass were weighed, 6 mL acetone was added and homogenized for 10 min with glass beads in a vortex. The samples were centrifuged (HERMLE Z300, New York, NY, USA) at 2500× *g* for 10 min until complete loss of the pellet or the supernatant color. The supernatant was analyzed using a spectrophotometer (Genesys 10S UV-VIS, Waltham, MA, USA) in the scanning spectrum (380 to 700 nm), and the resultant data by the Excel Add-In Solver on Windows 2013.

The content of carotenoids was determined based on Couso et al. [29]. Briefly, 10 mg of freeze-dried biomass was resuspended in methanol containing 0.03% of butylhydroxytoluene and homogenized for 3 minutes in a mixer mill (MM400, Retsch GmbH, Retsch-Alle 1-5, 42781 Haan, Germany), with glass beads and one tungsten bead, at 30 Hz, until complete loss of the pellet or the supernatant color. Then, the centrifuged extract was completely dried under nitrogen flow, and the pellet was resuspended in high-performance liquid chromatography (HPLC)-grade methanol and filtered (0.22 μm) into amber vials. The chromatographic analysis of the carotenoids was performed in a Prominence-i LC-2030Cplus (Shimadzu) HPLC equipped with a diode-array detector, using a column Surf C18 TriF100A 3μm 10 × 2.1 mm and a flow rate of 1 mL.min^{-1}. The mobile phase consisted of ethyl acetate as solvent A and 9:1 (*v:v*) acetonitrile:water as solvent B. The gradient program applied was: 0–16 min, 0–60% A; 16–30 min, 60% A; 30–32 min, 100% A, and 30–35 min 100% B. The injection volume was 100 μL, and the quantification was carried out at 450 nm using calibration curves of the neoxanthin, violaxanthin, lutein, and *β*-carotene standards. The respective calibration curves of pigment standards are supplied in Supplementary Materials (Table S1).

2.5. Statistical Analysis

For the design of experiments (DoE) assays, the statistical analysis of variance of Plackett–Burman was obtained with Minitab® v.20 software, and for Box–Behnken, the Design-Expert® v.11 software was used. The adequacy of the model was evaluated according to the correlation coefficient (R^2), *F*-test, and *p*-value, with a 95% of confidence level.

Regarding the experiments aside from DoE, statistical analyses were performed using R software version 3.6.1 in RStudio IDE version 1.2.1335. The mean and standard deviation were determined using biological triplicates for each experiment. The results were compared using one-way ANOVA, followed by Tukey-HSD multiple comparisons. Experimental results are presented with a 95% confidence level.

3. Results and Discussion

3.1. Preliminary Screening Using Plackett–Burman Design

The Plackett–Burman experimental layout was obtained with Minitab® v.20 software, and the respective results of the specific growth rates are described in Table S2 in Supplementary Materials. The results of the variance analysis are presented in Table 1.

Table 1. Statistical analysis of Plackett–Burman experiment for specific growth rates of heterotrophic cultures.

Factor	Low Level (−)	High Level (+)	Effect	t-Value	p-Value
Nitrogen source	$(NH_2)_2CO$	$(NH4)_2SO_4$	−0.006	−7.33	0.000
$(NH_2)_2CO$ $(NH_4)_2SO_4$	20.00 mM	60.00 mM	−0.002	−2.24	0.067
$NaH_2PO_4 \cdot H_2O$ + K_2HPO_4 *	10.00 mM	100.00 mM	−0.005	−6.05	0.001
$CaCl_2 \cdot 2H_2O$	1.00 mM	5.00 mM	0.000	0.45	0.667
$MgSO_4 \cdot 7H_2O$	1.00 mM	10.00 mM	−0.002	−2.43	0.051
$FeSO_4 \cdot 7H_2O$	0.05 mM	0.50 mM	0.001	1.69	0.142
$ZnSO_4 \cdot 7H_2O$	0.50 mM	2.50 mM	0.000	−0.08	0.935
$Cl_2Co \cdot 6H_2O$	0.00 mM	0.04 mM	0.000	−0.52	0.621
$Na_2MoO_4 \cdot 2H_2O$	0.00 mM	0.10 mM	0.000	−0.12	0.905
$MnSO_4 \cdot H_2O$	0.20 mM	1.50 mM	0.000	0.29	0.778
$NiCl_2 \cdot 6H_2O$	0.00 mM	0.02 mM	0.001	1.37	0.221
$CuSO_4 \cdot 5H_2O$	0.00 mM	0.02 mM	−0.002	−2.88	0.028
H_3BO_3	0.50 mM	1.50 mM	0.000	−0.44	0.673
Vitamins Mix **	0.5 dose	3 doses	0.000	0.22	0.835
Temperature	26 °C	30 °C	0.000	0.55	0.601

Model: $R^2 = 0.951$; $R_{adj}^2 = 0.827$; $R_{pred}^2 = 0.597$; p-value = 0.010; F-value = 7.70. * Na/K ratio = 3.24. ** Heterotrophic vitamins mix: Thiamine-HCl (1.0 g·L^{-1}), d-Biotin (0.015 g·L^{-1}), cyanocobalamin (B12) (0.012 g·L^{-1}), calcium pantothenate (0.030 g·L^{-1}) and PABA (*p*-Aminobenzoic acid) (0.060 g·L^{-1}). Dose: 1.50 mL·L^{-1}.

The nitrogen sources, $NaH_2PO_4 \cdot H_2O$ + K_2HPO_4, and $CuSO_4 \cdot 5H_2O$ were the statistically significant factors ($p < 0.05$) affecting the *C. amblystomatis* heterotrophic-specific growth rate, suggesting that the remaining factors were not limiting culture growth. Moreover, since the categoric factor registered a negative effect, the lower-level factor of $(NH_2)_2CO$ was the most appropriate nitrogen source.

The model registered a multiple correlation coefficient (R^2) of 0.951, indicating that more than 95% of the data in this screening could be explained by this model. Furthermore, an F-value of 7.70 and a p-value lower than 0.05 also support the significance of the model and the fit between the data and the model used.

3.2. Heterotrophic Medium Optimization Using Box–Behnken Design

Based on the previous results, a response surface methodology (Box–Behnken) was performed to determine the optimal values of $(NH_2)_2CO$, $NaH_2PO_4 \cdot H_2O$ + K_2HPO_4, and $CuSO_4 \cdot 5H_2O$, as well as their interactions to maximize *C. amblystomatis* heterotrophic specific growth rates.

The Box–Behnken layout, as well as the experimental and predicted results of specific growth rates, are shown in Table 2.

Table 2. Experimental layout of Box–Behnken design; the experimental and predicted results of the specific growth rates (μ) of heterotrophic cultures.

Run Order	$(NH_2)_2CO$ mM	$NaH_2PO_4 \cdot H_2O$ + K_2HPO_4 mM	$CuSO_4 \cdot 5H_2O$ mM	μ Experimental h^{-1}	μ Predicted h^{-1}
1	60	80	0.015	0.032	0.033
2	60	45	0.005	0.046	0.048
3	20	10	0.015	0.036	0.037
4	40	45	0.015	0.037	0.036
5	40	10	0.025	0.037	0.037
6	60	45	0.025	0.032	0.033
7	20	80	0.015	0.028	0.029
8	40	45	0.015	0.039	0.036
9	40	80	0.025	0.029	0.029
10	20	45	0.005	0.032	0.032
11	40	45	0.015	0.037	0.036
12	60	10	0.015	0.048	0.048
13	20	45	0.025	0.034	0.033
14	40	10	0.005	0.047	0.047
15	40	80	0.005	0.034	0.033

The 12th experiment (60 mM of $(NH_2)_2CO$, 10m M of $NaH_2PO_4 \cdot H_2O$ + K_2HPO_4 and 0.015 mM of $CuSO_4 \cdot 5H_2O$) registered the highest specific growth rate (0.048 h^{-1}), while the 7th experiment (20 mM of $(NH_2)_2CO$, 80 mM of $NaH_2PO_4 \cdot H_2O$ + K_2HPO_4 and 0.015 mM of $CuSO_4 \cdot 5H_2O$) resulted in the lowest value (0.028 h^{-1}).

The predicted results were obtained from the linear polynomial Equation (4), given by the model, as follows:

$$\begin{aligned} Specific\ growth\ rate &= 0.027707 + 0.000596[A] - 0.000124[B] + 0.291714[C] \\ &\quad -0.00000244306[A] \times [B] - 0.020235[A] \times [C] \\ &\quad +0.003894[B] \times [C] \end{aligned} \tag{4}$$

The statistical analysis, described in Table 3, demonstrated the $(NH_2)_2CO$, $NaH_2PO_4 \cdot H_2O$ + K_2HPO_4 and $CuSO_4 \cdot 5H_2O$ concentrations, as well as their interactions, which significantly affected ($p < 0.05$) *C. amblystomatis*-specific growth rate. The model registered a correlation coefficient R^2 of 0.980, suggesting the suitability of this model for predicting the responses in this experiment.

Table 3. Statistical analysis of Box–Behnken experiment for specific growth rates of heterotrophic cultures.

Source	Sum of Squares	Degree of Freedom	Mean Square	Coefficient Estimate	*F*-Value	*p*-Value
Model	0.0005	6	0.0001		65.25	<0.0001
A-$(NH_2)_2CO$	0.0001	1	0.0001	0.0034	76.66	<0.0001
B-$NaH_2PO_4 \cdot H_2O$ + K_2HPO_4	0.0003	1	0.0003	−0.0064	186.76	<0.0001
C-$CuSO_4 \cdot 5H_2O$	0.0001	1	0.0001	−0.0035	67.35	<0.0001
AB	0.0000	1	0.0000	−0.0010	8.40	0.0200
AC	0.0001	1	0.0001	−0.0042	47.02	0.0001
BC	0.0000	1	0.0000	0.0013	5.33	0.0498
Residual	0.0000	8	0.0000			
Lack of Fit	0.0000	6	0.0000		1.24	0.5107
Pure Error	0.0000	2	0.0000			
Corr. Total	0.0006	14				

Model: $R^2 = 0.980$; $R_{adj}^2 = 0.965$; $R_{pred}^2 = 0.937$.

Moreover, the interactions between $(NH_2)_2CO$, $NaH_2PO_4 \cdot H_2O$ + K_2HPO_4, and $CuSO_4 \cdot 5H_2O$ and specific growth rates (h^{-1}) were revealed by response surface plots (Figure 1). Varying the concentration of these factors causes a significant effect on the specific growth rates. According to the results, the model predicted the highest specific growth rates at approximately 60 mM of $(NH_2)_2CO$, 10 mM of $NaH_2PO_4 \cdot H_2O$ + K_2HPO_4 and 0.005 mM of $CuSO_4 \cdot 5H_2O$.
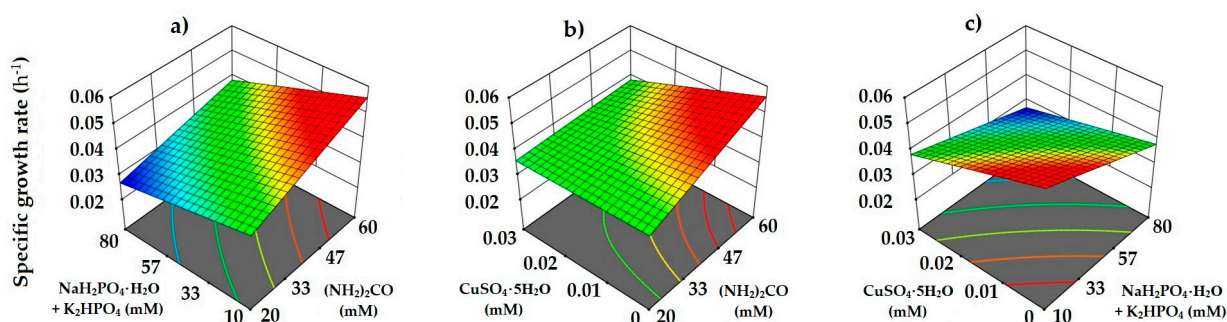
Figure 1. Response surface plots showing the interactions effects of (**a**) $(NH_2)_2CO$ and $NaH_2PO_4 \cdot H_2O$ + K_2HPO_4; (**b**) $CuSO_4 \cdot 5H_2O$ and $(NH_2)_2CO$, and (**c**) $CuSO_4 \cdot 5H_2O$ and $NaH_2PO_4 \cdot H_2O$ + K_2HPO_4 for the heterotrophic cultures.

Herewith, the final composition of the heterotrophic optimized medium was set as 60 mM of $(NH_2)_2CO$; 10 mM of $NaH_2PO_4 \cdot H_2O$ + K_2HPO_4; 3 mM of $CaCl_2 \cdot 2H_2O$; 5.50 mM of $MgSO_4 \cdot 7H_2O$; 0.30 mM of $FeSO_4 \cdot 7H_2O$; 1.50 mM of $ZnSO_4 \cdot 7H_2O$; 0.02 mM of $Cl_2Co \cdot 6H_2O$; 0.05 mM of $Na_2MoO_4 \cdot 2H_2O$; 0.85 mM of $MnSO_4 \cdot H_2O$; 0.005 mM of $CuSO_4 \cdot 5H_2O$; 1 mM of H_3BO_3; 0.01 mM of $NiCl_2 \cdot 6H_2O$ and 1 dose of heterotrophic vitamins mix (Thiamine-HCl (1.0 $g \cdot L^{-1}$), d-Biotin (0.015 $g \cdot L^{-1}$), cyanocobalamin (B12) (0.012 $g \cdot L^{-1}$), calcium pantothenate (0.030 $g \cdot L^{-1}$), and PABA (p-Aminobenzoic acid) (0.060 $g \cdot L^{-1}$). Dose: 1.50 $mL \cdot L^{-1}$).

3.3. Validation of Heterotrophic Medium Optimization

Hereupon, *C. amblystomatis* cultures grown with the company's heterotrophic basal medium were compared to those grown with the optimized heterotrophic medium (Table 4).

Table 4. Maximum and global volumetric productivities ($g \cdot L^{-1} \cdot h^{-1}$), specific growth rates (h^{-1}), and biomass production ($g \cdot L^{-1}$) of heterotrophic cultures grown using the company's basal medium and optimized medium. Different letters indicate significant differences between media. Values are given as means $\pm$ standard deviation ($n = 3$).

	Volumetric Productivity $g \cdot L^{-1} \cdot h^{-1}$		Specific Growth Rate h^{-1}	Biomass Production $g \cdot L^{-1}$
	Global	**Maximum**		
Basal medium	0.12 ± 0.01 [b]	0.29 ± 0.02 [b]	0.03 ± 0.00 [b]	7.71 ± 0.62 [b]
Optimized medium	0.19 ± 0.01 [a]	0.60 ± 0.06 [a]	0.05 ± 0.00 [a]	10.53 ± 0.59 [a]
% of increment	67.4	109.7	44.9	36.6

Cultures grown with the optimized medium registered an improvement of 44.9% in specific growth rate, from 0.034 to 0.050 h^{-1} ($p < 0.05$). Consequently, improvements of 67.4% were registered for global productivity, increasing from 0.12 to 0.19 $g \cdot L^{-1} \cdot h^{-1}$ ($p < 0.05$) and over 109.7% for maximum productivity, from 0.29 to 0.60 $g \cdot L^{-1} \cdot h^{-1}$ ($p < 0.05$). Furthermore, the highest biomass concentration of 10.53 $g \cdot L^{-1}$, in comparison to 7.66 $g \cdot L^{-1}$, was obtained from cultures grown with the optimized medium ($p < 0.05$). This appropriate culture medium recipe brought improvements in *C. amblystomatis* growth rates and productivity and resulted in higher cell concentrations, which is key to nutrient cost reduction and the operational costs of production in an industrial setting [18].

3.4. Photoautotrophic Medium Optimization Using Box–Behnken Design

Thereafter, a Box–Behnken design was performed for the photoautotrophic cultures based on the results obtained during the optimization of heterotrophic growth. The optimum nutrient concentration was diluted 10 times to fit the photoautotrophic growth requirements. Different nutrient concentrations were evaluated using half to double the amount of each class of nutrients to find the best proportion for this strain's photoautotrophic growth. "Other Macro" corresponds to the macronutrients $NaH_2PO_4 \cdot H_2O$ + K_2HPO_4, $CaCl_2 \cdot 2H_2O$, and $MgSO_4 \cdot 7H_2O$ and "Micro" corresponds to the micronutrients $FeSO_4 \cdot 7H_2O$, $ZnSO_4 \cdot 7H_2O$, $Cl_2Co \cdot 6H_2O$, $Na_2MoO_4 \cdot 2H_2O$, $MnSO_4 \cdot H_2O$, $NiCl_2 \cdot 6H_2O$, $CuSO_4 \cdot 5H_2O$, and H_3BO_3. The design layout and the respective specific growth rate, experimental, and predicted results are described in Table 5.

Table 5. Experimental layout of the Box–Behnken design and the results of the experimental and predicted specific growth rates (μ) of the photoautotrophic cultures.

Run Order	[Urea] Times	[Other Macro] Times	[Micro] Times	μ Experimental d^{-1}	μ Predicted d^{-1}
1	1.25	0.50	2.00	0.30	0.30
2	2.00	0.50	1.25	0.34	0.34
3	0.50	1.25	2.00	0.29	0.28
4	1.25	1.25	1.25	0.31	0.31
5	1.25	0.50	0.50	0.35	0.34
6	1.25	1.25	1.25	0.31	0.31
7	1.25	2.00	2.00	0.29	0.29
8	0.50	1.25	0.50	0.27	0.27
9	0.50	0.50	1.25	0.28	0.29
10	1.25	1.25	1.25	0.32	0.31

Table 5. *Cont.*

Run Order	[Urea] Times	[Other Macro] Times	[Micro] Times	μ Experimental d^{-1}	μ Predicted d^{-1}
11	1.25	2.00	0.50	0.31	0.32
12	2.00	1.25	2.00	0.27	0.27
13	0.50	2.00	1.25	0.28	0.28
14	2.00	2.00	1.25	0.31	0.30
15	2.00	1.25	0.50	0.35	0.35

According to the results, the 5th and the 15th experiments offered the highest specific growth rates (0.35 d^{-1}), while the 8th and 12th experiments registered the lowest specific growth rate (0.27 d^{-1}).

The predicted results were obtained from the quadratic Equation (5), given by the model as follows:

$$
\begin{aligned}
Specific~growth~rate \\
= 0.198540 + 0.166906[A] - 0.024934[B] + 0.052475[C] \\
-0.015188[A] \times [B] - 0.042049[A] \times [C] \\
+0.007058[B] \times [C] - 0.028010\big[A^2\big] + 0.008854\big[B^2\big] \\
-0.011739\big[C^2\big]
\end{aligned}
\tag{5}
$$

The statistical analysis described in Table 6 demonstrates that urea, other macro- and micronutrients, and the interaction between urea and micronutrients were significant factors affecting the culture's specific growth rate ($p < 0.05$). Moreover, the model registered a correlation coefficient R^2 of 0.969, suggesting that this model was suitable for predicting the responses in this experiment.

Table 6. Statistical analysis of Box–Behnken experiment for specific growth rates of photoautotrophic cultures.

Source	Sum of Squares	Degrees of Freedom	Mean Square	Coefficient Estimate	*F*-Value	*p*-Value
Model	0.0093	9	0.0010		17.07	0.0030
A-Urea	0.0029	1	0.0029	0.0190	47.53	0.0010
B-Other Macronutrients	0.0008	1	0.0008	−0.0097	12.44	0.0168
C-Micronutrients	0.0019	1	0.0019	−0.0155	31.46	0.0025
AB	0.0003	1	0.0003	−0.0085	4.80	0.0799
AC	0.0022	1	0.0022	−0.0237	36.82	0.0018
BC	0.0001	1	0.0001	0.0040	1.04	0.3552
A^2	0.0009	1	0.0009	−0.0158	15.08	0.0116
B^2	0.0001	1	0.0001	0.0050	1.51	0.2743
C^2	0.0002	1	0.0002	−0.0066	2.65	0.1645
Residual	0.0003	5	0.0001			
Lack of Fit	0.0001	3	0.0000		0.39	0.7775
Pure Error	0.0002	2	0.0001			
Corr. Total	0.0096	14				

Model: $R^2 = 0.969$; $R_{\text{adj}}^2 = 0.912$; $R_{\text{pred}}^2 = 0.770$.

Additionally, the interactions between urea, other macronutrients, and the micronutrients and the specific growth rates were revealed by response surface plots (Figure 2).
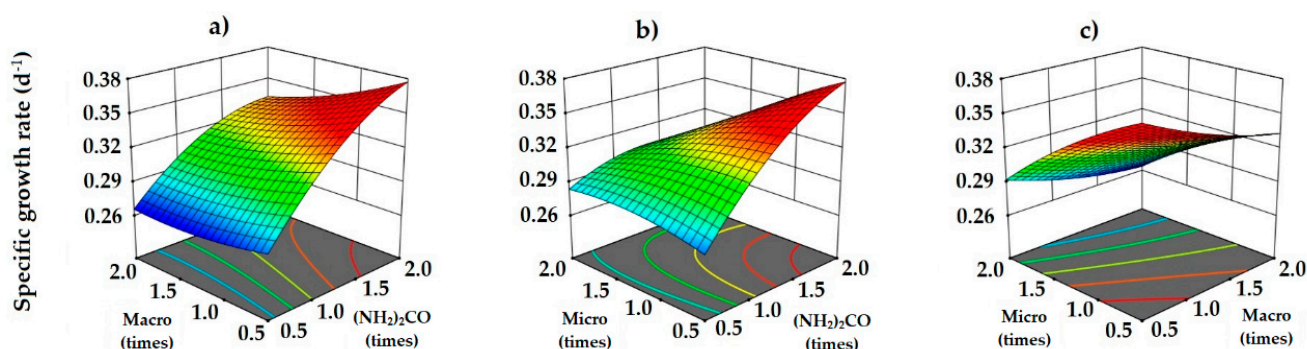

Figure 2. Response surface plots showing the interaction effects of (**a**) other macronutrients (Macro) and $(NH_2)_2CO$; (**b**) micronutrients (Micro) and $(NH_2)_2CO$, and (**c**) Macro and Micro of the photoautotrophic cultures.

According to the results, the model predicted the highest specific growth rate using two times the concentration of urea, and half the concentration of other macronutrients and micronutrients.

Herewith, the final composition of the photoautotrophic optimized medium was set as 12 mM of $(NH_2)_2CO$; 0.50 mM of $NaH_2PO_4 \cdot H_2O$ + K_2HPO_4; 0.15 mM of $CaCl_2 \cdot 2H_2O$; 0.275 mM of $MgSO_4 \cdot 7H_2O$; 0.015 mM of $FeSO_4 \cdot 7H_2O$; 0.075 mM of $ZnSO_4 \cdot 7H_2O$; 0.001 mM of $Cl_2Co \cdot 6H_2O$; 0.0025 mM of $Na_2MoO_4 \cdot 2H_2O$; 0.0425 mM of $MnSO_4 \cdot H_2O$; 0.00025 mM of $CuSO_4 \cdot 5H_2O$; 0.05 mM of H_3BO_3; 0.0005 mM of $NiCl_2 \cdot 6H_2O$, and 1 dose of photoautotrophic vitamins mix (Thiamine-HCl (350 mg·L^{-1}), d-Biotin (50 mg·L^{-1}), cyanocobalamin (B12) (30 mg·L^{-1}). Dose: 0.5 mL·L^{-1}).

3.5. Validation of Photoautotrophic Medium Optimization

Afterwards, *C. amblystomatis* cultures grown with the company's photoautotrophic basal medium were compared to those grown with the resultant photoautotrophic optimized medium. The biomass volumetric productivities, specific growth rates, and biomass production are described in Table 7.

Table 7. Maximum and overall volumetric productivity (g·L^{-1}·d^{-1}), specific growth rate (d^{-1}), and biomass production (g·L^{-1}) of the photoautotrophic cultures grown with the company's basal medium and optimized medium in 1 L bubble columns. Different letters indicate significant differences between media. Values are given as mean ± standard deviation (*n* = 3).

	Volumetric Productivity g·L^{-1}·d^{-1}		Specific Growth Rate d^{-1}	Biomass Production g·L^{-1}
	Global	**Maximum**		
Basal medium	0.12 ± 0.00 [b]	0.17 ± 0.01 [b]	0.23 ± 0.01 [b]	1.36 ± 0.02 [b]
Optimized medium	0.19 ± 0.01 [a]	0.27 ± 0.02 [a]	0.35 ± 0.01 [a]	1.91 ± 0.06 [a]
% of increment	55.8	65.8	51.2	40.8

Cultures grown with the optimized medium registered a higher specific growth rate (0.35 d^{-1}) compared to those grown with the basal medium (0.23 d^{-1}), offering an improvement of 51.2%. Moreover, 55.8% and 65.8% improvements were registered for global and maximum productivity, respectively. Cultures grown with the optimized medium also achieved a higher maximum biomass concentration (1.91 g·L^{-1}) compared to that obtained with the basal medium, which reached 1.36 g·L^{-1}, enabling an improvement of 40.8%.

3.6. Biochemical Composition

3.6.1. Proximate Composition

The proteins, lipids, carbohydrates, and ashes contents were determined to further characterize the biochemical composition of the biomass resultant from both heterotrophic and photoautotrophic media optimization (Table 8).

Table 8. Proximate composition of biomass with hetero- and photoautotrophic basal and optimized media. Proteins, lipids, carbohydrates, and ashes are presented as the percentage of the biomass dry weight. Different letters indicate significant differences between media. Values are given as means ± standard deviation (*n* = 3).

	Medium	Proteins (%)	Lipids (%)	Carbohydrates (%)	Ashes (%)
Hetero.	Basal	33.49 ± 0.38 [d]	7.41 ± 1.89 [c]	47.68 ± 2.19 [a]	11.42 ± 0.07 [c]
	Optimized	61.49 ± 0.13 [b]	8.88 ± 0.70 [c]	14.11 ± 0.58 [b]	15.52 ± 0.24 [b]
Photoauto.	Basal	56.67 ± 1.06 [c]	19.74 ± 1.07 [a]	4.26 ± 0.47 [c]	19.39 ± 1.53 [a]
	Optimized	73.45 ± 1.91 [a]	13.28 ± 0.45 [b]	8.23 ± 0.02 [c]	6.07 ± 0.07 [d]

Proteins are the main product of several microalgal-based biorefineries [30]. Microalgae proteins are high quality since these micro-organisms can synthesize all the essential amino acids and also have functional biological activities with increased human health benefits [4,31,32]. Furthermore, algal sources of protein are largely used as feed additive in aquaculture [8]. The cultures grown with the optimized media registered the highest protein contents, 61.49–73.45% dry weight (DW) (*p* < 0.05). Therefore, *C. amblystomatis* might strengthen the microalgal protein market, which is expected to cover 50% of the total alternative protein market by 2054 [33].

The lowest carbohydrate content was registered in the photoautotrophic cultures (*p* < 0.05). The cells grown with a heterotrophic-optimized medium contained a much lower content of carbohydrates (14.11% of DW) than those obtained from cultures grown with heterotrophic basal medium (47.68% of DW). In microalgae, the high content of carbohydrates might be stored under unfavorable conditions at the expense of proteins [32,34], which can also explain the low content of protein in the cultures grown with the heterotrophic basal medium.

The cultures grown in heterotrophy registered the lowest lipid content (7.41–8.88% of DW) (*p* < 0.05). The highest content was achieved in the cultures grown with de basal photoautotrophic medium: 19.74% of DW, which is in concordance with the results reported for this microalga [35]: 18.33% of DW, using the same cultivation medium in a 2.5 m^3 closed tubular photobioreactor.

The ash contents were also similar to those reported for this microalga [35] (9.88–15.85% of DW), being the lowest value registered in the cultures grown with the optimized photoautotrophic medium (6.07% of DW) (*p* < 0.05).

3.6.2. Fatty Acids Profile

In order to evaluate the lipid composition, the fatty acid methyl esters (FAME) profile was analyzed (Table 9). FAME contents below 0.50% of total fatty acids were excluded.

Table 9. Fatty acid methyl esters (FAME) profile; presented in percentage of total fatty acids of *Chlorococcum amblystomatis* biomass grown with hetero- and photoautotrophic basal and optimized media. Different letters indicate significant differences between media. Values are given as mean ± standard deviation (*n* = 3).

FAME %	Heterotrophy		Photoautotrophy	
	Basal	Optimized	Basal	Optimized
C14:0	0.88 ± 0.05 [a]	0.66 ± 0.03 [b]	0.66 ± 0.00 [b]	nd
C16:4*n*-3	14.09 ± 0.14 [b]	18.63 ± 1.509 [a]	15.07 ± 0.40 [b]	14.88 ± 0.12 [b]
C16:3*n*-3	nd	1.10 ± 0.38 [a]	1.31 ± 0.07 [a]	1.14 ± 0.03 [a]
C16:2*n*-6	2.38 ± 0.08 [b]	1.68 ± 0.03 [c]	1.23 ± 0.10 [d]	3.12 ± 0.23 [a]
C16:1	9.68 ± 0.33 [a]	5.50 ± 0.33 [b]	1.21 ± 0.19 [c]	1.77 ± 0.94 [c]
C16:0	30.95 ± 0.38 [a]	32.33 ± 1.51 [a]	23.25 ± 0.16 [b]	22.35 ± 0.76 [b]
C17:3	5.07 ± 0.22 [a]	4.32 ± 0.20 [b]	2.71 ± 0.10 [c]	3.06 ± 0.18 [c]
C18:4*n*-3	2.56 ± 0.03 [d]	5.03 ± 0.15 [b]	6.03 ± 0.35 [a]	3.49 ± 0.29 [c]
C18:3*n*-3	nd	nd	34.26 ± 0.20 [a]	28.46 ± 0.38 [b]
C18:3*n*-6	8.10 ± 0.11 [b]	10.30 ± 0.09 [a]	4.47 ± 0.04 [d]	5.27 ± 0.06 [c]
C18:2*n*-6	12.26 ± 0.62 [a,b]	10.59 ± 0.56 [b]	5.38 ± 0.19 [c]	13.38 ± 0.79 [a]
C18:1	11.46 ± 0.06 [a]	7.58 ± 3.71 [a,b]	2.05 ± 0.02 [b,c]	1.54 ± 0.05 [c]
C18:0	2.55 ± 0.53 [a]	2.29 ± 0.14 [a,b]	2.03 ± 0.11 [a,b]	1.52 ± 0.19 [b]
Σ SFA	34.39 ± 0.29 [a]	35.28 ± 1.67 [a]	26.27 ± 0.48 [b]	23.87 ± 0.94 [b]
Σ MUFA	21.14 ± 0.37 [a]	13.08 ± 4.01 [a]	3.27 ± 0.20 [b]	3.31 ± 0.89 [b]
Σ PUFA	44.47 ± 0.57 [c]	51.64 ± 2.37 [b]	70.46 ± 0.63 [a]	72.82 ± 0.07 [a]
Σ *n*-3	16.66 ± 0.15 [d]	24.76 ± 2.02 [c]	56.68 ± 0.38 [a]	47.26 ± 0.62 [b]
Σ *n*-6	22.74 ± 0.75 [a]	22.57 ± 0.55 [a]	11.07 ± 0.29 [b]	21.78 ± 0.56 [a]
Σ*n*-6/Σ*n*-3	1.37 ± 0.06 [a]	0.92 ± 0.05 [b]	0.20 ± 0.00 [d]	0.45 ± 0.02 [c]
PUFA/SFA	1.29 ± 0.03 [c]	1.46 ± 0.02 [c]	2.68 ± 0.07 [b]	3.06 ± 0.12 [a]

nd: not detected.

The dominant FAME in the heterotrophic cultures of *C. amblystomatis* was C16:0 (30.95–32.33% of total fatty acids; TFA), while in the photoautotrophic cultures, it was C18:3*n*-3 (28.46–34.26% of TFA), which was not detected in the heterotrophic cultures. The second most abundant FAME was C16:4*n*-3 (14.09–18.635% of TFA), followed by C18:2*n*-6 (5.38–13.38% of TFA), C18:3*n*-6 (4.47–10.30% of TFA), C18:1 (1.54–11.46% of TFA), and C16:1 (1.21–9.68% of TFA). The remaining FAME values were similar between the cultures grown in both the hetero- and photoautotrophic conditions.

Furthermore, the prevalent polyunsaturated fatty acids (PUFAs) were more abundant in the photoautotrophic cultures (70.46–72.82% of TFA) compared to the heterotrophically grown cultures (44.47–51.64% of TFA). On the contrary, monosaturated fatty acids (MUFA) displayed higher concentrations in heterotrophic biomass (13.08–21.14% of TFA) compared to the photoautotrophic cultures (3.27–3.31% of TFA; $p < 0.05$). Lastly, the amount of saturated fatty acids (SFA) was slightly higher in heterotrophic cultures (34.39–35.28% of TFA) in comparison to the photoautotrophic ones (23.87–26.27% of TFA).

The Σ*n*-6/Σ*n*-3 ratio plays an important role in human health, being recommended by the World Health Organization to be lower than 10 to prevent a negative impact on human health since *n*-6 PUFAs are pro-inflammatory whereas *n*-3 PUFAs are anti-inflammatory [36,37]. All hetero- and photoautotrophic cultures registered a Σ*n*-6/Σ*n*-3 ratio from 0.2 to 1.37 and more PUFA content in comparison to SFAs (with PUFA/SFA ratio above 1, from 1.29 to 3.06). Thereby, *C. amblystomatis* might represent an interesting source of PUFAs.

3.6.3. Chlorophylls and Carotenoids Contents

The content of carotenoids and chlorophylls of *C. amblystomatis* was evaluated (Table 10).

Table 10. Pigment profile in mg·g^{-1} of *Chlorococcum amblystomatis* biomass grown with hetero- and photoautotrophic basal and optimized heterotrophic media. Different letters indicate significant differences between media. Values are given as mean ± standard deviation (*n* = 3).

Pigments (mg·g^{-1})	Heterotrophy		Photoautotrophy	
	Basal	Optimized	Basal	Optimized
Neoxanthin	0.52 ± 0.05 [c]	0.79 ± 0.06 [c]	1.46 ± 0.12 [b]	3.66 ± 0.33 [a]
Violaxanthin	0.02 ± 0.00 [c]	0.06 ± 0.01 [c]	0.51 ± 0.03 [b]	0.75 ± 0.06 [a]
Lutein	1.23 ± 0.10 [c]	1.60 ± 0.11 [c]	4.32 ± 0.15 [b]	5.27 ± 0.37 [a]
β-carotene	0.81 ± 0.16 [b]	4.15 ± 0.22 [a]	5.37 ± 0.44 [a]	5.84 ± 0.98 [a]
Chlorophyll *a* and *b*	8.53 ± 0.35 [c]	14.59 ± 0.74 [b]	12.88 ± 0.61 [b]	29.32 ± 0.39 [a]

Pigments are high-value products that are synthesized naturally under photoautotrophic conditions. Nevertheless, some pigments can be produced in heterotrophic dark conditions but at lower concentrations [11,38]. Thereby, as expected, the *C. amblystomatis* cultures grown in heterotrophic conditions registered a decreased content of pigments globally compared to cultures grown in photoautotrophic conditions (*p* < 0.05), except for *β*-carotene.

C. amblystomatis registered lower chlorophyll content values than those previously reported (40.24 mg·g^{-1} in 2.5 m^3 tubular photobioreactor) [35]. Under heterotrophic growth, this microalga registered 8.53–14.59 mg·g^{-1} of chlorophyll *a* and *b*, and under photoautotrophy, they registered 12.88–29.32 mg·g^{-1}. Chlorophylls are mainly used as a natural food dye and have several reported human health benefits due to their antioxidant and anti-inflammatory properties [38,39]. Besides chlorophylls, carotenoids are the second most abundant pigment group [11]. The main carotenoids in the *C. amblystomatis* profile were lutein and β-carotene, with 1.23–1.60 mg·g^{-1} and 4.32–5.27 mg·g^{-1} of lutein, and 0.81–4.15 mg·g^{-1} and 5.37–5.84 mg·g^{-1} of β-carotene in heterotrophy and photoautotrophy, respectively. Carotenoids are strong antioxidants and have been described to prevent several cardiovascular and neurodegenerative diseases, cancer, diabetes, and macular degeneration [40]. β-carotene plays an important role in human nutrition because it acts as provitamin A, being converted into vitamin A in vivo [41,42]. Vitamin A deficiency represents a global problem in developing countries, and it is related to human visual malfunction and decreased immune function [41,43]. Lutein is among the most important carotenoids in the human diet (as a food colorant) and prevents macular degeneration [43,44]. *C. amblystomatis* registered high lutein content, similar to the main lutein producers *Muriellopsis* sp. (4.3 mg·g^{-1}) and *Scenedesmus almeriensis* (4.5 mg·g^{-1}) [45]. The main application of microalgae as lutein producers is as feed additive in aquaculture [44,45] and poultry livestock.

C. amblystomatis also registered a high content of neoxanthin in the cultures grown with optimized photoautotrophic medium (3.66 mg·g^{-1}). Neoxanthin was reported to significantly reduce the risk of prostate cancer, proving to be one of the strongest carotenoids with antiproliferative effects on human prostate cancer cells [46].

Finally, it is worth mentioning that the global carotenoids market size had already reached USD 1.44 billion in 2019 and is expected to rise to USD 1.84 billion by 2027 [47]. Indeed, higher demand for natural sources of pigments has been observed over the last years, and, therefore, *C. amblystomatis* presents great pigment content even without any biosynthesis induction, which is promising in the context of these market opportunities.

4. Conclusions

Medium optimization through surface response methodology revealed increments of 44.9–51.2% in *Chlorococcum amblystomatis*-specific growth rates and 36.6–40.8% in biomass production under heterotrophy and photoautotrophy, respectively. Heterotrophic cultivation registered a 5.5-fold increase in biomass production compared to photoautotrophic cultivation at the laboratory scale, supporting the two-stage approach for further industrial

high-quality biomass production with a reduced scale-up time. Moreover, optimizing the cultivation medium towards biomass production has shown significant differences in the biochemical composition of the resultant biomass in comparison to the biomass obtained from the basal media cultivation. The optimized biomass revealed an interesting composition that is rich in protein (61.49–73.45% of dry weight (DW)), registering higher content than those reported for the biomass obtained from the basal media (33.49–56.67% of DW) in heterotrophy and photoautotrophy, respectively, representing an alternative protein source. *C. amblystomatis* was also demonstrated to be a promising source of polyunsaturated fatty acids (51.64–72.82% of total fatty acids) and might be a natural food colorant due to its high carotenoids content (1.60–5.27 mg·g^{-1} of DW of lutein and 4.15–5.84 mg·g^{-1} of DW of β-carotene) in heterotrophic and photoautotrophic optimized biomasses, respectively, being a sustainable alternative as a source of nutrients to address the increasing world food and feed demands.

References

1. Pulz, O.; Gross, W. Valuable products from biotechnology of microalgae. *Appl. Microbiol. Biotechnol.* **2004**, *65*, 635–648. [CrossRef]
2. Hlaing, S.A.A.; Sadiq, M.B.; Anal, A.K. Enhanced yield of Scenedesmus obliquus biomacromolecules through medium optimization and development of microalgae based functional chocolate. *J. Food Sci. Technol.* **2020**, *57*, 1090–1099. [CrossRef]
3. Priyadarshani, I.; Rath, B. Commercial and industrial applications of micro algae—A review. *J. Algal Biomass Util.* **2012**, *3*, 89–100.
4. Ejike, C.E.; Collins, S.A.; Balasuriya, N.; Swanson, A.K.; Mason, B.; Udenigwe, C.C. Prospects of microalgae proteins in producing peptide-based functional foods for promoting cardiovascular health. *Trends Food Sci. Technol.* **2017**, *59*, 30–36. [CrossRef]
5. Caporgno, M.P.; Mathys, A. Trends in Microalgae Incorporation Into Innovative Food Products With Potential Health Benefits. *Front. Nutr.* **2018**, *5*, 58. [CrossRef] [PubMed]
6. Rumin, J.; Junior, R.G.D.O.; Bérard, J.-B.; Picot, L. Improving Microalgae Research and Marketing in the European Atlantic Area: Analysis of Major Gaps and Barriers Limiting Sector Development. *Mar. Drugs* **2021**, *19*, 319. [CrossRef] [PubMed]
7. de Medeiros, V.P.B.; da Costa, W.K.A.; da Silva, R.T.; Pimentel, T.C.; Magnani, M. Microalgae as source of functional ingredients in new-generation foods: Challenges, technological effects, biological activity, and regulatory issues. *Crit. Rev. Food Sci. Nutr.* **2021**, *62*, 4929–4950. [CrossRef] [PubMed]
8. Spolaore, P.; Joannis-Cassan, C.; Duran, E.; Isambert, A. Commercial applications of microalgae. *J. Biosci. Bioeng.* **2006**, *101*, 87–96. [CrossRef]

9. Barros, A.; Pereira, H.; Campos, J.; Marques, A.; Varela, J.; Silva, J. Heterotrophy as a tool to overcome the long and costly autotrophic scale-up process for large scale production of microalgae. *Sci. Rep.* **2019**, *9*, 13935. [CrossRef]

10. Daneshvar, E.; Ok, Y.S.; Tavakoli, S.; Sarkar, B.; Shaheen, S.M.; Hong, H.; Luo, Y.; Rinklebe, J.; Song, H.; Bhatnagar, A. Insights into upstream processing of microalgae: A review. *Bioresour. Technol.* **2021**, *329*, 124870. [CrossRef]

11. Hu, J.; Nagarajan, D.; Zhang, Q.; Chang, J.-S.; Lee, D.-J. Heterotrophic cultivation of microalgae for pigment production: A review. *Biotechnol. Adv.* **2018**, *36*, 54–67. [CrossRef]

12. Bumbak, F.; Cook, S.; Zachleder, V.; Hauser, S.; Kovar, K. Best practices in heterotrophic high-cell-density microalgal processes: Achievements, potential and possible limitations. *Appl. Microbiol. Biotechnol.* **2011**, *91*, 31–46. [CrossRef]

13. Perez-Garcia, O.; Escalante, F.M.E.; De-Bashan, L.E.; Bashan, Y. Heterotrophic cultures of microalgae: Metabolism and potential products. *Water Res.* **2011**, *45*, 11–36. [CrossRef] [PubMed]

14. Chen, G.-Q.; Chen, F. Growing Phototrophic Cells without Light. *Biotechnol. Lett.* **2006**, *28*, 607–616. [CrossRef] [PubMed]

15. Ogbonna, J.C.; Masui, H.; Tanaka, H. Sequential heterotrophic/autotrophic cultivation-An efficient method of producing Chlorella biomass for health food and animal feed. *J. Appl. Phycol.* **1997**, *9*, 359–366. [CrossRef]

16. Dionisi, H.M.; Lozada, M.; Olivera, N.L. Bioprospection of marine microorganisms: Biotechnological applications and methods. *Rev. Argent Microbiol.* **2012**, *44*, 49–60. [CrossRef]

17. Pandey, M.K.; Dasgupta, C.N.; Mishra, S.; Srivastava, M.; Gupta, V.K.; Suseela, M.R.; Ramteke, P.W. Bioprospecting microalgae from natural algal bloom for sustainable biomass and biodiesel production. *Appl. Microbiol. Biotechnol.* **2019**, *103*, 5447–5458. [CrossRef]

18. Fábregas, J.; Domínguez, A.; Regueiro, M.; Maseda, A.; Otero, A. Optimization of culture medium for the continuous cultivation of the microalga Haematococcus pluvialis. *Appl. Microbiol. Biotechnol.* **2000**, *53*, 530–535. [CrossRef]

19. Mandenius, C.-F.; Brundin, A. Review: Biocatalysts and bioreactor design Bioprocess Optimization Using Design-of-Experiments Methodology. *Biotechnol. Prog.* **2008**, *24*, 1191–1203. [CrossRef] [PubMed]

20. Cheng, K.-C.; Demirci, A.; Catchmark, J.M. Enhanced pullulan production in a biofilm reactor by using response surface methodology. *J. Ind. Microbiol. Biotechnol.* **2010**, *37*, 587–594. [CrossRef]

21. Sarabia, L.A.; Ortiz, M.C. Response Surface Methodology. *Compr. Chemom.* **2009**, *1*, 345–390. [CrossRef]

22. Steinberg, D.M.; Bursztyn, D. Response Surface Methodology in Biotechnology. *Qual. Eng.* **2010**, *22*, 78–87. [CrossRef]

23. Chen, J.; Lan, X.; Jia, R.; Hu, L.; Wang, Y. Response Surface Methodology (RSM) Mediated Optimization of Medium Components for Mycelial Growth and Metabolites Production of Streptomyces alfalfae XN-04. *Microorganisms* **2022**, *10*, 1854. [CrossRef] [PubMed]

24. Chlorococcum Amblystomatis (F.D.Lambert ex N.Wille) N.Correia, J.Varela & Leonel Pereira: AlgaeBase. Available online: https://www.algaebase.org/search/species/detail/?species_id=175845 (accessed on 16 September 2022).

25. Bligh, E.G.; Dyer, W.J. A rapid method of total lipid extraction and purification. *Can. J. Biochem. Physiol.* **1959**, *37*, 911–917. [CrossRef]

26. Pereira, H.; Barreira, L.; Mozes, A.; Florindo, C.; Polo, C.; Duarte, C.V.; Custódio, L.; Varela, J. Microplate-based high throughput screening procedure for the isolation of lipid-rich marine microalgae. *Biotechnol. Biofuels* **2011**, *4*, 61. [CrossRef]

27. Nunez, M.; Quigg, A. Changes in growth and composition of the marine microalgae phaeodactylum tricornutum and nannochloropsis salina in response to changing sodium bicarbonate concentrations. *J. Appl. Phycol.* **2016**, *28*, 2123–2138. [CrossRef]

28. Lepage, G.; Roy, C.C. Improved recovery of fatty acid through direct transesterification without prior extraction or purification. *J. Lipid Res.* **1984**, *25*, 1391–1396. [CrossRef] [PubMed]

29. Couso, I.; Vila, M.; Vigara, J.; Cordero, B.F.; Vargas, M.; Rodríguez, H.; León, R. Synthesis of carotenoids and regulation of the carotenoid biosynthesis pathway in response to high light stress in the unicellular microalga Chlamydomonas reinhardtii. *Eur. J. Phycol.* **2012**, *47*, 223–232. [CrossRef]

30. Chew, K.W.; Yap, J.Y.; Show, P.L.; Suan, N.H.; Juan, J.C.; Ling, T.C.; Lee, D.-J.; Chang, J.-S. Microalgae biorefinery: High value products perspectives. *Bioresour. Technol.* **2017**, *229*, 53–62. [CrossRef]

31. Guedes, A.C.; Malcata, F.X. Nutritional Value and Uses of Microalgae in Aquaculture. *Aquaculture* **2012**, *10*, 59–78. [CrossRef]

32. Becker, E.W. Micro-algae as a source of protein. *Biotechnol. Adv.* **2007**, *25*, 207–210. [CrossRef]

33. Khanra, S.; Mondal, M.; Halder, G.; Tiwari, O.; Gayen, K.; Bhowmick, T.K. Downstream processing of microalgae for pigments, protein and carbohydrate in industrial application: A review. *Food Bioprod. Process.* **2018**, *110*, 60–84. [CrossRef]

34. Del Río, E.; García-Gómez, E.; Moreno, J.; Guerrero, M.G.; García-González, M. Microalgae for oil. Assessment of fatty acid productivity in continuous culture by two high-yield strains, Chlorococcum oleofaciens and Pseudokirchneriella subcapitata. *Algal Res.* **2017**, *23*, 37–42. [CrossRef]

35. Correia, N.; Pereira, H.; Silva, J.T.; Santos, T.; Soares, M.; Sousa, C.B.; Schüler, L.M.; Costa, M.; Varela, J.; Pereira, L.; et al. Isolation, Identification and Biotechnological Applications of a Novel, Robust, Free-living Chlorococcum (Oophila) amblystomatis Strain Isolated from a Local Pond. *Appl. Sci* **2020**, *10*, 3040. [CrossRef]

36. Pereira, H.; Barreira, L.; Figueiredo, F.; Custódio, L.; Vizetto-Duarte, C.; Polo, C.; Rešek, E.; Engelen, A.; Varela, J. Polyunsaturated fatty acids of marine macroalgae: Potential for nutritional and pharmaceutical applications. *Mar. Drugs* **2012**, *10*, 1920–1935. [CrossRef] [PubMed]

37. Schmitz, G.; Ecker, J. The opposing effects of n-3 and n-6 fatty acids. *Prog. Lipid Res.* **2008**, *47*, 147–155. [CrossRef] [PubMed]

38. Morales-Sánchez, D.; A Martinez-Rodriguez, O.; Martinez, A. Heterotrophic cultivation of microalgae: Production of metabolites of commercial interest. *J. Chem. Technol. Biotechnol.* **2017**, *92*, 925–936. [CrossRef]

39. Balder, H.F.; Vogel, J.; Jansen, M.C.; Weijenberg, M.P.; van den Brandt, P.A.; Westenbrink, S.; Van Der Meer, R.; Goldbohm, R.A. Heme and chlorophyll intake and risk of colorectal cancer in the Netherlands cohort study. *Cancer Epidemiol. Biomark. Prev.* **2006**, *15*, 717–725. [CrossRef]

40. Paiva, S.A.R.; Russell, R.M. Beta-carotene and other carotenoids as antioxidants. *J. Am. Coll. Nutr.* **1999**, *18*, 426–433. [CrossRef]

41. Tang, G.; Russell, R.M. Carotenoids as Provitamin, A. *Carotenoids* **2009**, *5*, 149–172. [CrossRef]

42. Chen, B.H.; Chuang, J.R.; Lin, J.H.; Chiu, C.P. Quantification of Provitamin A Compounds in ChInese Vegetables by High-Performance Liquid Chromatography. *J. Food Prot.* **1993**, *56*, 51–54. [CrossRef] [PubMed]

43. Mostafa, S.S.M. Microalgal Biotechnology: Prospects and Applications. *Plant Sci.* **2012**, *12*, 276–314. [CrossRef]

44. Fernández-Sevilla, J.M.; Fernández, F.A.; Grima, E.M. Biotechnological production of lutein and its applications. *Appl. Microbiol. Biotechnol.* **2010**, *86*, 27–40. [CrossRef] [PubMed]

45. Del Campo, J.A.; García-González, M.; Guerrero, M.G. Outdoor cultivation of microalgae for carotenoid production: Current state and perspectives. *Appl. Microbiol. Biotechnol.* **2007**, *74*, 1163–1174. [CrossRef] [PubMed]

46. Kotake-Nara, E.; Asai, A.; Nagao, A. Neoxanthin and fucoxanthin induce apoptosis in PC-3 human prostate cancer cells. *Cancer Lett.* **2005**, *220*, 75–84. [CrossRef] [PubMed]

47. Market Research Report. Available online: https://www.fortunebusinessinsights.com/industry-reports/carotenoids-market-100180 (accessed on 19 December 2022).